Simulation of the mechanical behavior of a rubber pumping system under large deformations.

Author: Ing. Andrea Romeo
LPA
Consorzio per la promozione della cultura plastica
Proplast
Str. Comunale Savonesa, 9
Rivalta Scrivia (AL)
Italy
+39 01311859743
www.proplast.it

Simulation of the mechanical behavior of a rubber pumping system under large deformations.

An exploration on the mechanical behavior of a highly deformed rubber component through FE analysis is performed via the definition of the best material model suitable. In order to consider non linearity of material, elastic-plastic and hyperelastic models are investigated and simulation results are compared to experimental tests. Accurate prevision on deformed shape has been achieved by software simulation also in the large deformation domain although the system considered is highly non-linear (geometric, contact and material non-linearity).
The hyperelastic approach has provided acceptable accordance in the description of global force needs and energy absorption of the system during deformation. Due to the complexity of the physical phenomena involved, the hyperelastic approach –and the Radioss material model used as well- appears suitable of improvement and enhancement via a more accurate material characterization taking into account strain rate and thermal dependence, visco-elastic behavior in time and cyclic hysteresis.

Author: Ing. Andrea Romeo
LPA
Consorzio per la promozione della cultura plastica
Proplast
Str. Comunale Savonesa, 9
Rivalta Scrivia (AL)
Italy
+39 01311859743
www.proplast.it

proplast
PLASTICS INNOVATION POLE

1. Simulation of rubber components:

Via FEM simulations an effort to predict the behaviour of **rubber components** in the large deformations domain is important in many industrial and civil applications.

Critical matters are:

- High non linearity of the elastic behaviour (hyperelasticity);
- Cyclic behaviour (Mullins effect, hysteresis)

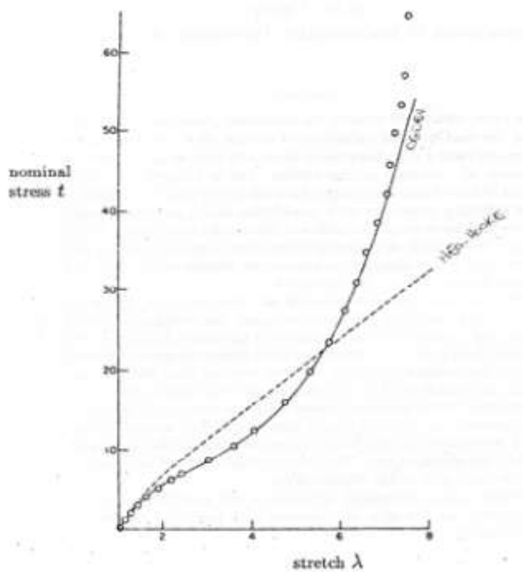

hyperelasticity

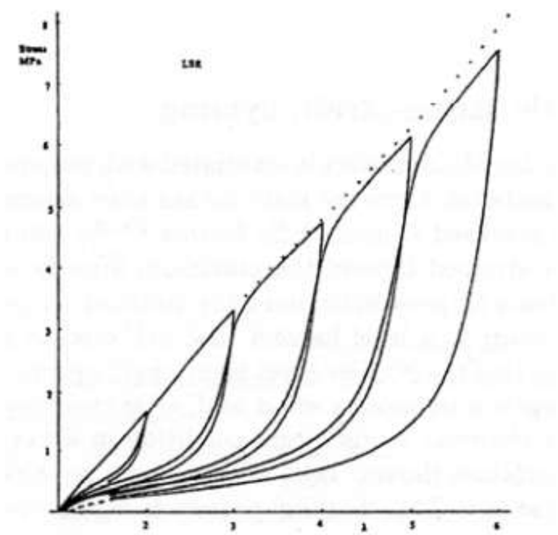

Mullins effect

1. Case study

Rubber pumping system for dispenser of cosmetic, perfume or house-cleaning products.

Material: thermoplastic polyester compound TPE-E (Hytrel 4068).

Activities:

- Component design;
- Prototype mould design and construction;
- Experimental testing on the prototype (plate compression and mandrel compression);
- Material characterization;
- FEM simulations using Radioss;
- Benchmark of results (deformed shape and working force for both loading and unloading phase).

Experimental testing

2. Plate compression testing:

Plate stroke: 10 mm;

Strain rate: 100 mm/min;

N° of cycles: 20 loading and unloading cycles.

<u>1st cycle</u>

Max applied loading force: 24.1 N

Min applied unloading force: 8.5 N

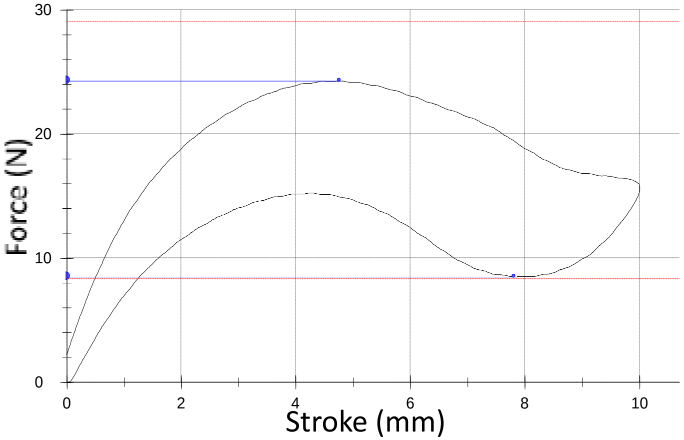

<u>20th cycle</u>

Max applied loading force: 18.3 N

Min applied unloading force: 8.1 N

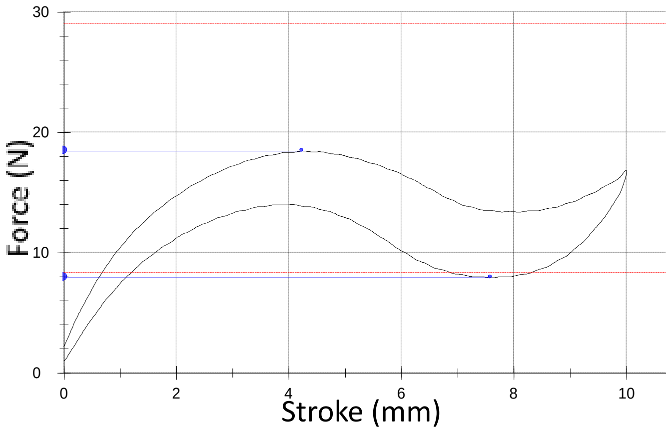

2. Plate compression testing:

A reduction on the applied force is shown with the number of cycle both for the max loading force (23%) and the min unloading force (5%).

An asymptotic trend is achieved from the 10^{th} cycle on.

A good repeatability of the test is seen testing a number of specimens.

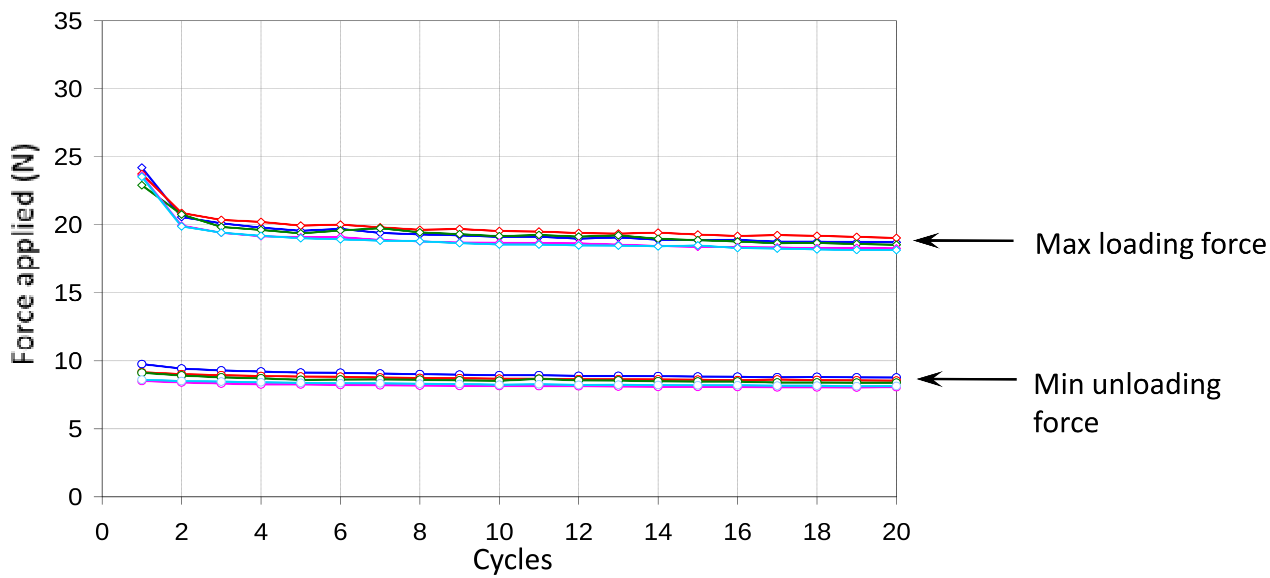

Material characterization on standard Dumbell specimens under cyclic stress in conditions similar to the testing ones (100 mm/min).

For a better description of the regime behaviour, Stress-strain curves used for simulations <u>will be those of the 10^{th} cycle</u>.

FEM simulations

3.1 Material description – elastoplastic model

Preliminary set of analysis:

- elasto-plastic material model (Law 36 in Radioss);
- axysimmetric model;
- Imposed displacement of the lower nodes.

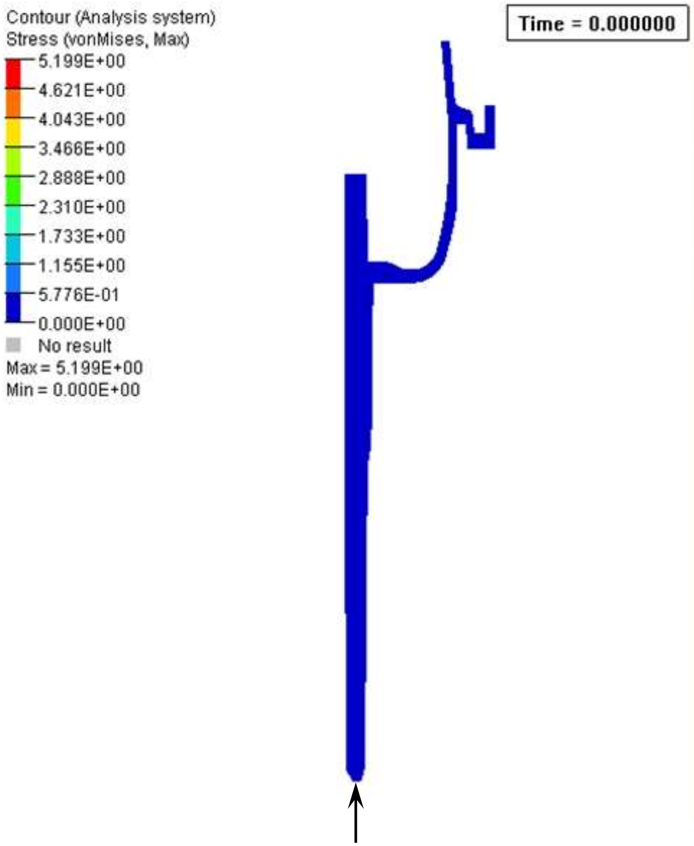

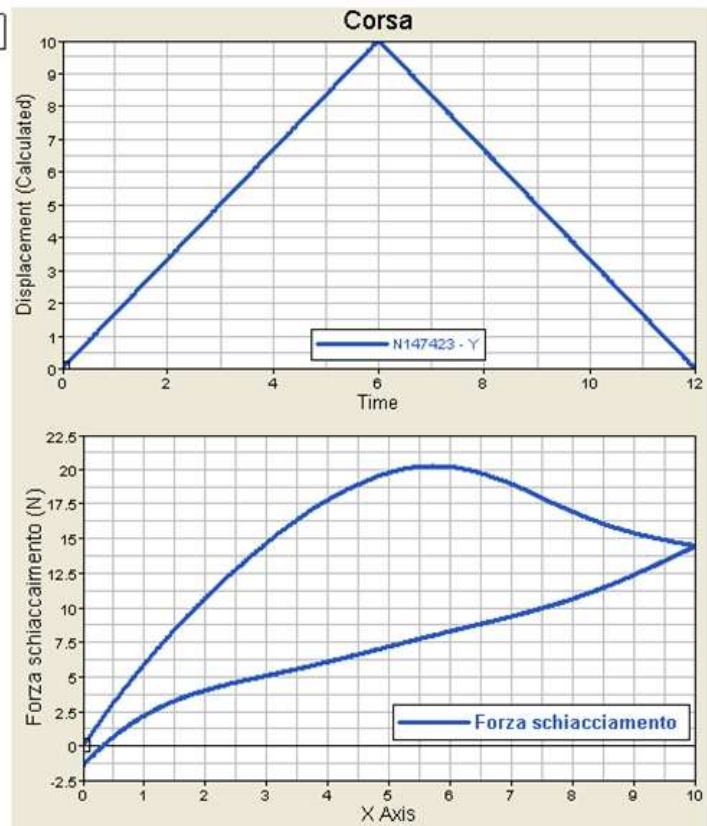

3.1 Material description – elastoplastic model

Results:

- Good approximation for the loading phase if compared to the experimental testing;
- Poor accordance to the experimental data for the unloading phase (due to high material non-linearity that is not taken into account by the material model used);
- Lower value of the max applied force in comparison to the experimental testing.

Experimental data

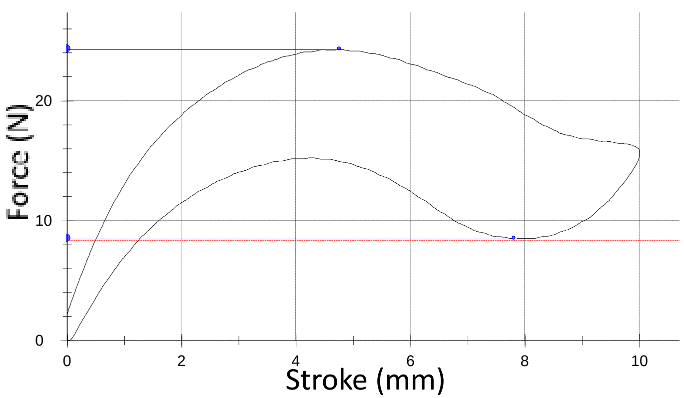

Max applied loading force: 24.1 N

Simulation

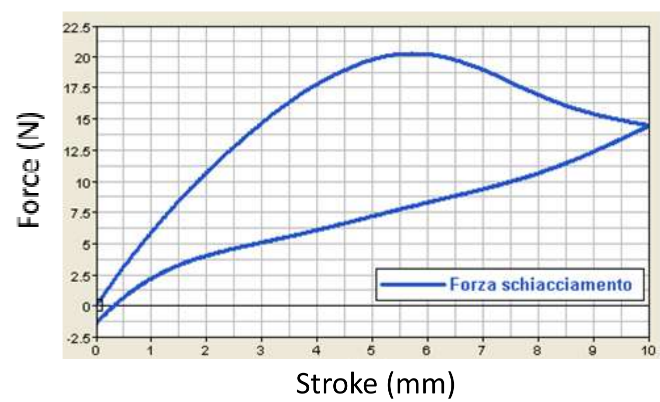

Max applied loading force: 20.9 N (-13 %)

3.2 Material description – hyperelastic model

Second set of analysis:

- Hyperelastic material models: Mooney Rivlin and Ogden (3rd order) (Law 42 in Radioss);

$$W = \sum_{i=1}^{N} \frac{\mu_i}{\alpha_i}(\lambda_1^{\alpha_i} + \lambda_2^{\alpha_i} + \lambda_3^{\alpha_i} - 3)$$

Potential deformation Energy (Ogden Formulation for uncompressible elastomers)

Where: $\lambda_i = 1 + \varepsilon_i$ Principal stretches

Thus, known $W = W(\boldsymbol{\lambda})$ → $\sigma_i = \lambda_i \frac{\partial W}{\partial \lambda_i}$ Principal Cauchy stresses

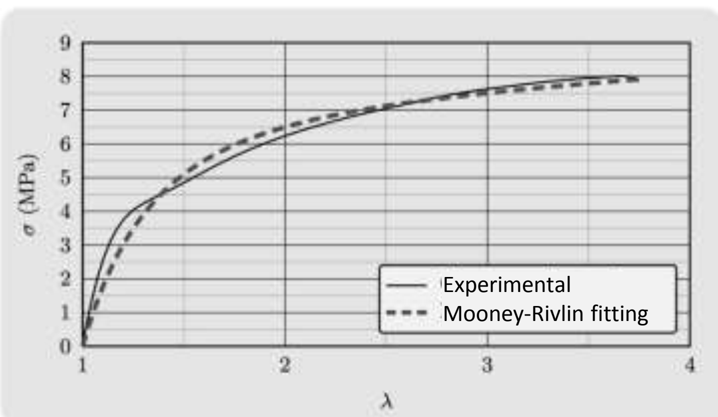

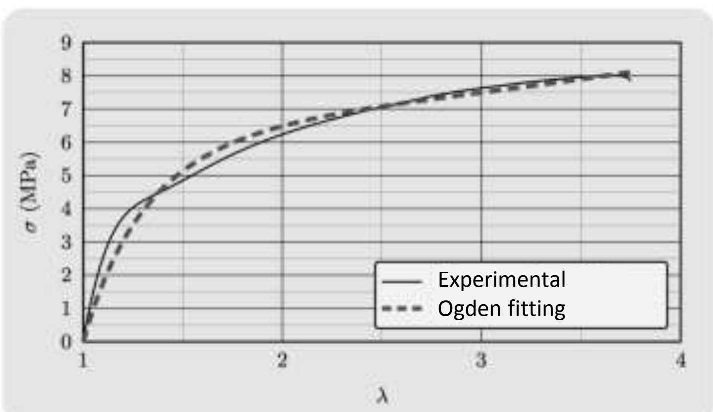

$C_{10} = 0.18$

$C_{01} = 3.34$

Mooney-Rivlin

$\mu_1 = 279.39$	$\alpha_1 = -0.03$
$\mu_2 = 0.20$	$\alpha_2 = 2.83$
$\mu_3 = -11.53$	$\alpha_3 = -1.42$

~~**Ogden**~~

3.2 Material description – hyperelastic model

Results:

- Better approximation for the loading phase if compared to the elasto-plastic model;
- No prevision on the unloading phase (because this is a purely elastic model and unloading is going to be exactly coincident with loading).
- Lower value of the max applied force in comparison to the experimental testing.

Experimental data

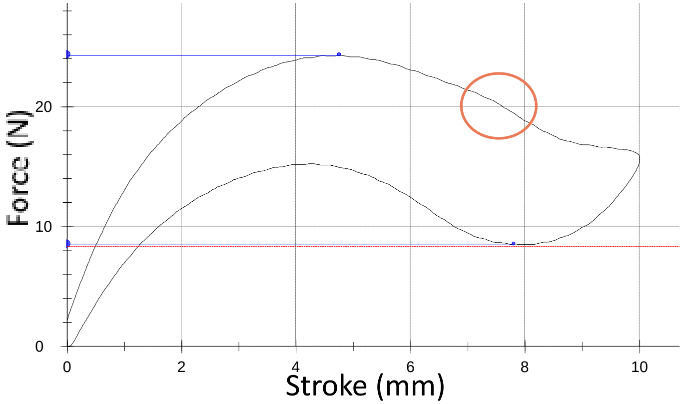

Simulation

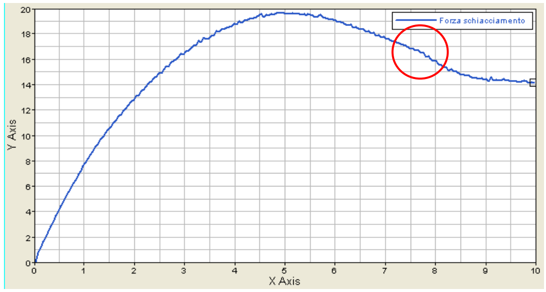

Max applied loading force: 24.1 N

Max applied loading force: 19.9 N (-17 %)

3.2 Material description – hyperelastic model

Results:

- Good prevision of the deformed shape obtained by the solid (brick) model.

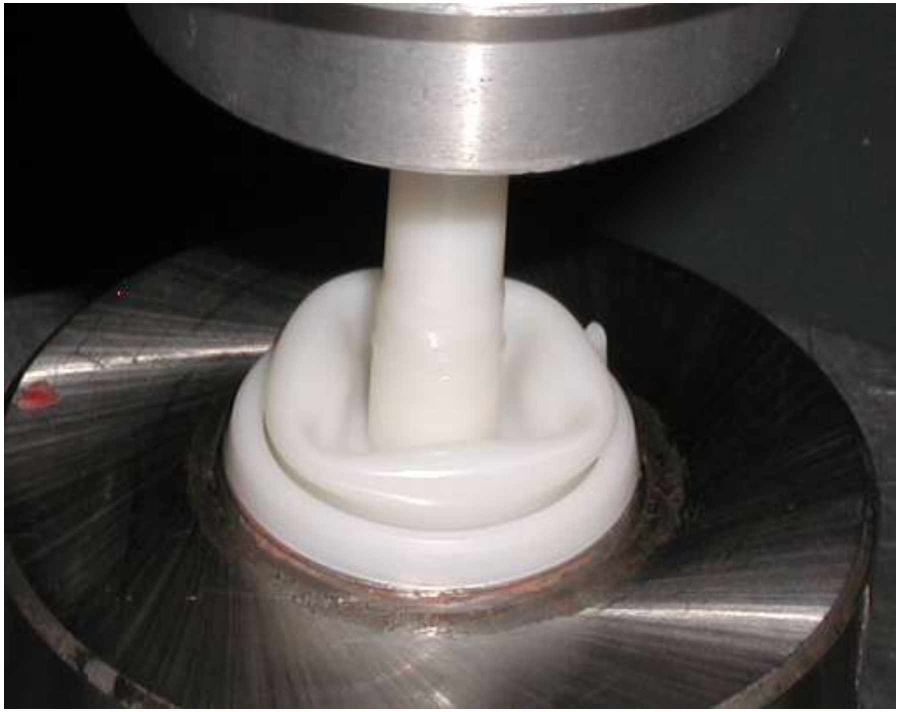

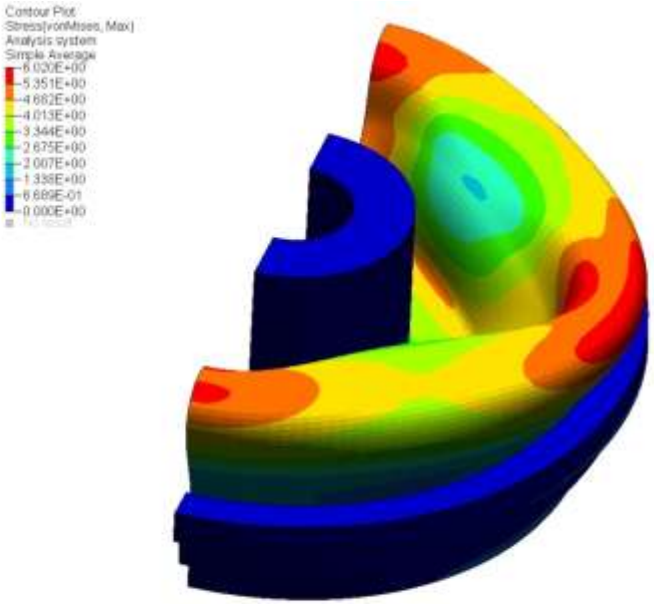

3.3 Material description – elastomer model

Third set of analysis:

- Elastomer model (Law 65 in Radioss);
- Different curves tabulated for loading and unloading taking into account hysteresis;
- Shell model (the material model at the moment is available only for shells):
    - Discretization and manual input of thicknesses (introduces errors into the model);
- Characterization on standard ISO specimen under cyclic uniaxial tension. (minimum preload).

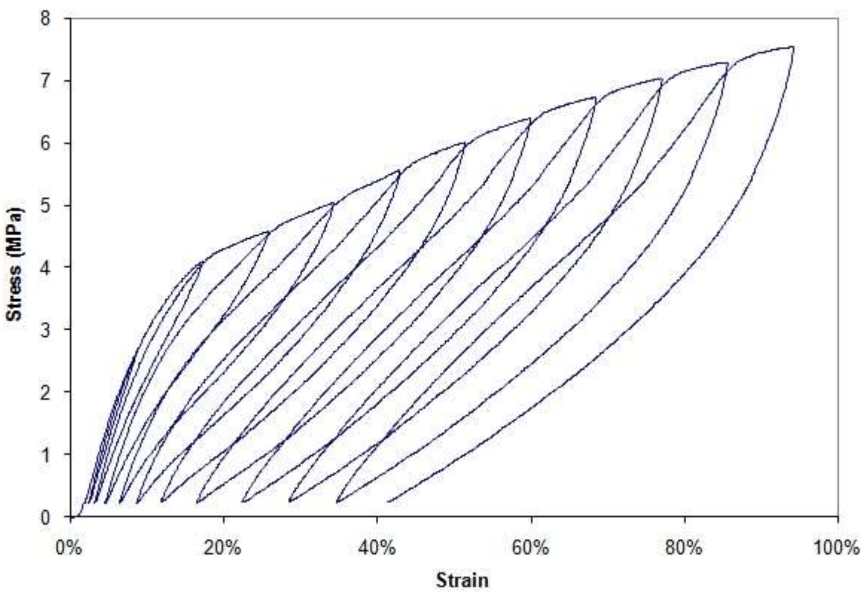

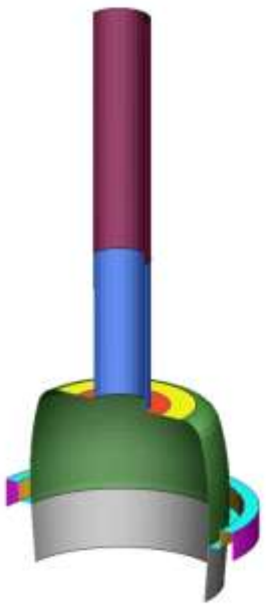

3.3 Material description – elastomer model

Results:

- Prevision of both loading and unloading phases;
- The simulated force-displacement curve shows the same qualitative trend as the experimental data (maximum of the applied force both in loading and unloading phase).
- Numerical values of the applied force are to be improved through a better description of the shell model (mesh refinement and thickness determination) and of the unloading material characterization.

Experimental data

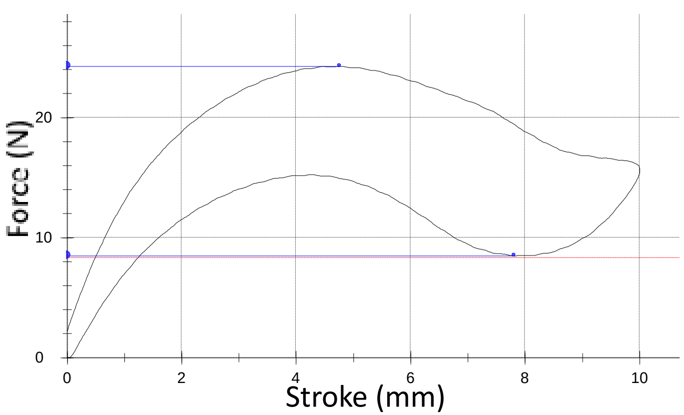

Max applied loading force: 24.1 N

Simulation

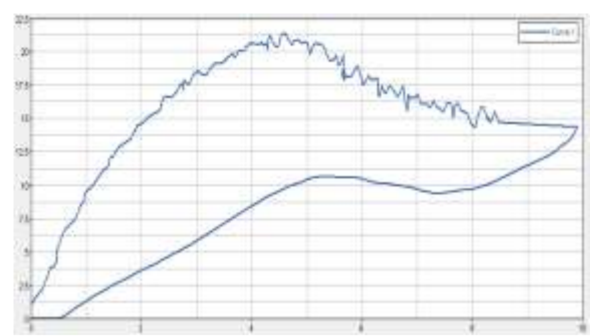

Max applied loading force: 20.7 N (-14 %)

Conclusions

4. Conclusions

1. A description of the mechanical behaviour of the elastomeric component was possible through FEM analysis.
2. Due to the complexity of the phenomena involved some different material models (availablein Radioss) were used, each better describing a particular aspect (loading or unloading phases, force applied, deformed shape etc.).

3. The **elastoplastic** (law 36) axysimmetric model yielded a slightly more accurate prevision of the maximum loading force applied but poor accordance in the unloading phase.
4. The **hyperelastic** (law 42) solid (brick) model was used to improve the description of the shape of the force-displacement curve for the loading phase but was not suitable to study the unloading phase.
5. The "**elastomer**" (law 65) shell model allowed to describe both the loading and unloading pashes showing a qualitatively correct behaviour with local maximums in the F-d curve for the loading and the unloading phase, as well. Improvements in the shell model can be achieved as far as the shell model is concerned. Thus, a more accurate thickness determination and mesh refinement would improve the correspondence between experimental and simulated results.

4. Conclusions

6. The problem appears to be worth of further investigation. In particular the “elastomer” Radioss material model (law 65) seems to be very powerful and versatile in description of rubber components under large deformations.

7. Improvements in the hyperelastic model (law 42) are desirable with the introduction of any damage parameter or hysteresis factor for describing the energy loss due to elastomeric behaviour under cyclic load.

8. The deformed shape is very well predicted by both the solid and shell models.

9. The numerical prediction of force and energy consumption is also strongly affected by the material characterization. Other testing should be performed (shear, biaxial tension, compression) and implemented in the FE models.